ChemPubSoc Europe
DOI: 10.1002/chem.201903007
CHEMISTRY A European Journal Communicatio

Radicals

Luminescent Mono-, Di-, and Triradicals: Bridging Polychlorinated Triarylmethyl Radicals by Triarylamines and Triarylboranes

Yohei Hattori,[a] Evripidis Michail,[a] Alexander Schmiedel,[a] Michael Moos,[a] Marco Holzapfel,[a] Ivo Krummenacher,[b] Holger Braunschweig,[b] Ulrich Müller,[c] Jens Pflaum,[c] and Christoph Lambert*[a]

Abstract: Up to three polychlorinated pyridyldiphenylmethyl radicals bridged by a triphenylamine carrying electron withdrawing (CN), neutral (Me), or donating (OMe) groups were synthesized and analogous radicals bridged by tris(2,6-dimethylphenyl)borane were prepared for comparison. All compounds were as stable as common closed-shell organic compounds and showed significant fluorescence upon excitation. Electronic, magnetic, absorption, and emission properties were examined in detail, and experimental results were interpreted using DFT calculations. Oxidation potentials, absorption and emission energies could be tuned depending on the electron density of the bridges. The triphenylamine bridges mediated intramolecular weak antiferromagnetic interactions between the radical spins, and the energy difference between the high spin and low spin states was determined by temperature dependent ESR spectroscopy and DFT calculations. The fluorescent properties of all radicals were examined in detail and revealed no difference for high and low spin states which facilitates application of these dyes in two-photon absorption spectroscopy and OLED devices.

Introduction

Organic π-radicals or radical ions are typically nonemitting species. Among several molecules that "violate" this rule[1] are donor-acceptor compounds comprising chlorinated triphenylmethyl radicals as electron acceptors in combination with arylamine donors.[2] Emission in the red to near infrared spectral region with sizable quantum yields have been reported. Furthermore, for compounds with carbazole as the donor efficient OLEDs could be fabricated.[3]

The topology of the triphenylmethyl radical and the triphenylamine donor also allowed the synthesis of linear oligomers,[4] polymers[5] and branched chromophores[6] that show charge transfer upon optical excitation. However, while radicals are useful building blocks for functional materials,[7] almost nothing is known about the luminescent properties of such di- and polyradicals.[8] Thus, the focus of this work is to elucidate the basic emission properties of di- and triradicals based on polychlorinated pyridyldiphenylmethyl radical as the spin bearing unit, to compare them with suitable monoradical parent compounds, and to demonstrate some potential applications in OLEDs and as two-photon absorption chromophores. A particular focus will lie on the modification of the bridge moiety connecting the two (or three) radical centers and its impact on the optical performance.

Results and Discussion

In this study, the polychlorinated pyridyldiphenylmethyl radical (PyBTM″) is combined with a triarylamine bridge. In our design of the compounds, three, two, or one PyBTM″ moieties are bonded to the 4, 4′, and 4″ positions of triphenylamine (TPA) and the remaining free positions are filled with cyano, methyl or methoxy groups in order to tune the donor strength of the triarylamine (see Figure 1). Compared to the previously used perchlorinated triphenylmethyl and tris(trichlorophenyl)methyl radicals, where the chlorine atoms serve to enhance the acceptor character and, concomitantly, shield the radical center to make it persistent, the polychlorinated pyridyldiphenylmethyl radical is distinctly less light sensitive,[1e,9] an issue which is quite important for any (electro)optical application. Thus, **TPA(PyBTM″)$_3$** triradical, **TPA(CN)(PyBTM″)$_2$**, **TPA(Me)(PyBTM″)$_2$**, **TPA(OMe)(PyBTM″)$_2$** diradicals, and **TPA(CN)$_2$(PyBTM″)**, **TPA(Me)$_2$(PyBTM″)**, **TPA(OMe)$_2$(PyBTM″)** monoradicals were syn-

[a] Dr. Y. Hattori, E. Michail, A. Schmiedel, M. Moos, Dr. M. Holzapfel, Prof. C. Lambert
Institute of Organic Chemistry, Julius-Maximilians-University Würzburg
Am Hubland, 97074 Würzburg (Germany)
E-mail: christoph.lambert@uni-wuerzburg.de

[b] Dr. I. Krummenacher, Prof. H. Braunschweig
Institute of Inorganic Chemistry, Julius-Maximilians-University Würzburg
Am Hubland, 97074 Würzburg (Germany)

[c] U. Müller, Prof. J. Pflaum
Institute of Physics, Julius-Maximilians-University Würzburg
Am Hubland, 97074 Würzburg (Germany)

Supporting information and the ORCID identification number(s) for the author(s) of this article can be found under: https://doi.org/10.1002/chem.201903007.

© 2019 The Authors. Published by Wiley-VCH Verlag GmbH & Co. KGaA. This is an open access article under the terms of Creative Commons Attribution NonCommercial License, which permits use, distribution and reproduction in any medium, provided the original work is properly cited and is not used for commercial purposes.

 © 2019 The Authors. Published by Wiley-VCH Verlag GmbH & Co. KGaA, Weinheim

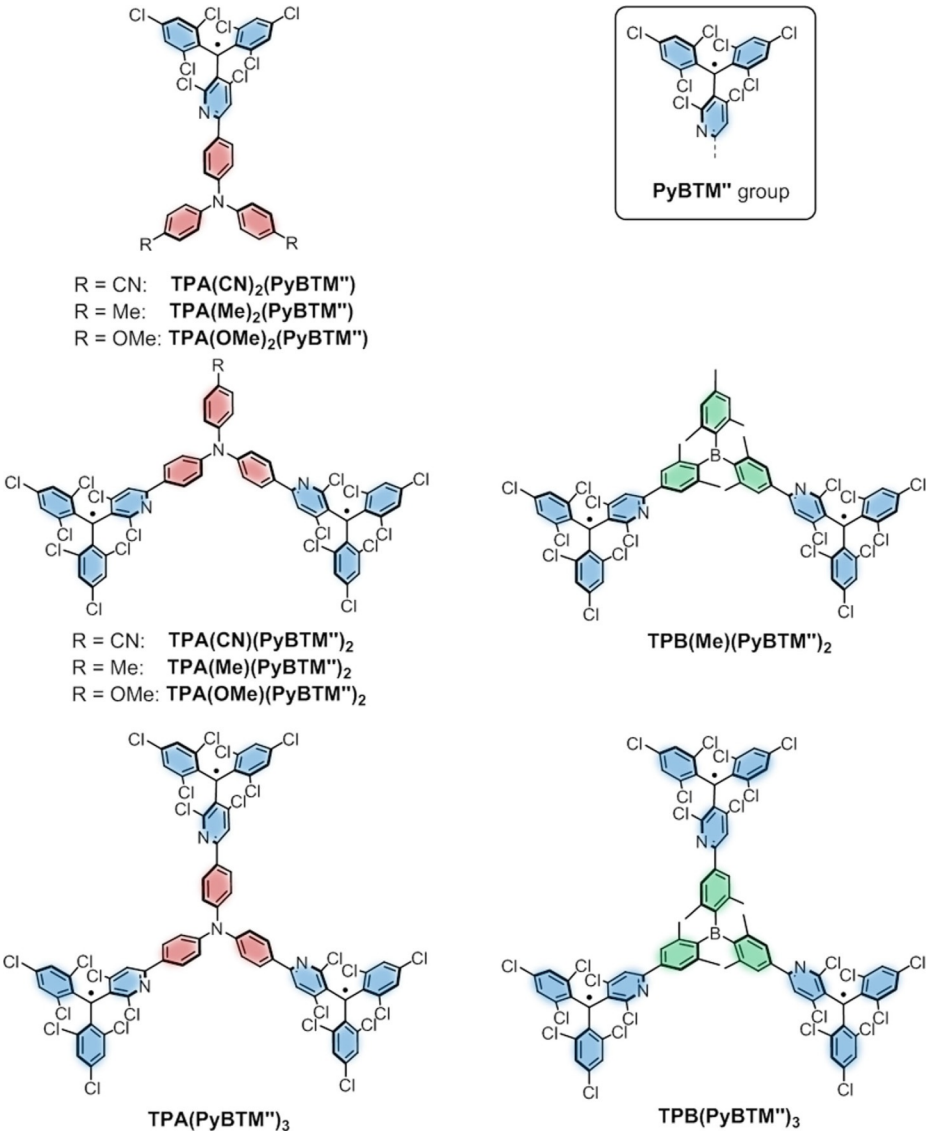

Figure 1. Structures of mono-, di-, triradicals.

thesized (Figure 1, see also the Supporting Information). In order to compare the donor bridge with an acceptor bridge,[10] we also prepared tris(2,6-dimethylphenyl)borane (TPB) compounds, **TPB(PyBTM″)$_3$** triradical and **TPB(Me)(PyBTM″)$_2$** diradical.[11]

For estimating the donor strength of the bridging triarylamine group we measured cyclic voltammograms of the radicals (Figure S6, Table S3). These show the reduction waves of the PyBTM″ groups at around −0.9 V (vs. Fc^+/Fc). While for the TPB compounds the first oxidation waves at +0.74 V (vs. Fc^+/Fc) refer to the PyBTM″ groups, the TPA compounds show the first oxidation wave in a less oxidative region (+0.20–0.57 V vs. Fc^+/Fc) which corresponds to the oxidation of the triarylamine group. First oxidation of TPA rather than PyBTM″ can be judged from the ratios of the oxidation to reduction waves (1:1 for monoradicals, 1:2 for diradicals, 1:3 for triradicals) in addition to the expectation of the oxidation potentials. The phenomenon that another group is oxidized before the radical group is called "SOMO-HOMO energy-level conversion".[12] The order of oxidation susceptibility, **TPA(OMe)$_2$(PyBTM″)** > **TPA(Me)$_2$(PyBTM″)** > **TPA(OMe)(PyBTM″)$_2$** > **TPA(Me)(PyBTM″)$_2$** > **TPA(PyBTM″)$_3$** > **TPA(CN)(PyBTM″)$_2$** > **TPA(CN)$_2$(PyBTM″)** reflects the electron donating ability of the TPA along the substituent R = OMe > Me > PyBTM″ > CN.

The ground and excited spin doublet states are unique characteristics of monoradicals. For the spin multiplicities of the di- or triradicals, orientation of two or three spins have to be considered. Diradicals can possess triplet (high spin, HS, ferromagnetic coupling of spin centers) or singlet states (low spin, LS, antiferromagnetic coupling), and triradicals can adopt quartet (HS) or doublet (LS) states.

In order to estimate the magnetic interaction between the radical centers in the ground state, temperature dependent EPR spectra were measured for the di- and triradicals in frozen toluene. In addition to $g = 2$ signals, half-field transitions typical of triplet states were observed for the diradicals as well as for the quartet states of triradicals (see Figure 2a and Figure S2).

 © 2019 The Authors. Published by Wiley-VCH Verlag GmbH & Co. KGaA, Weinheim

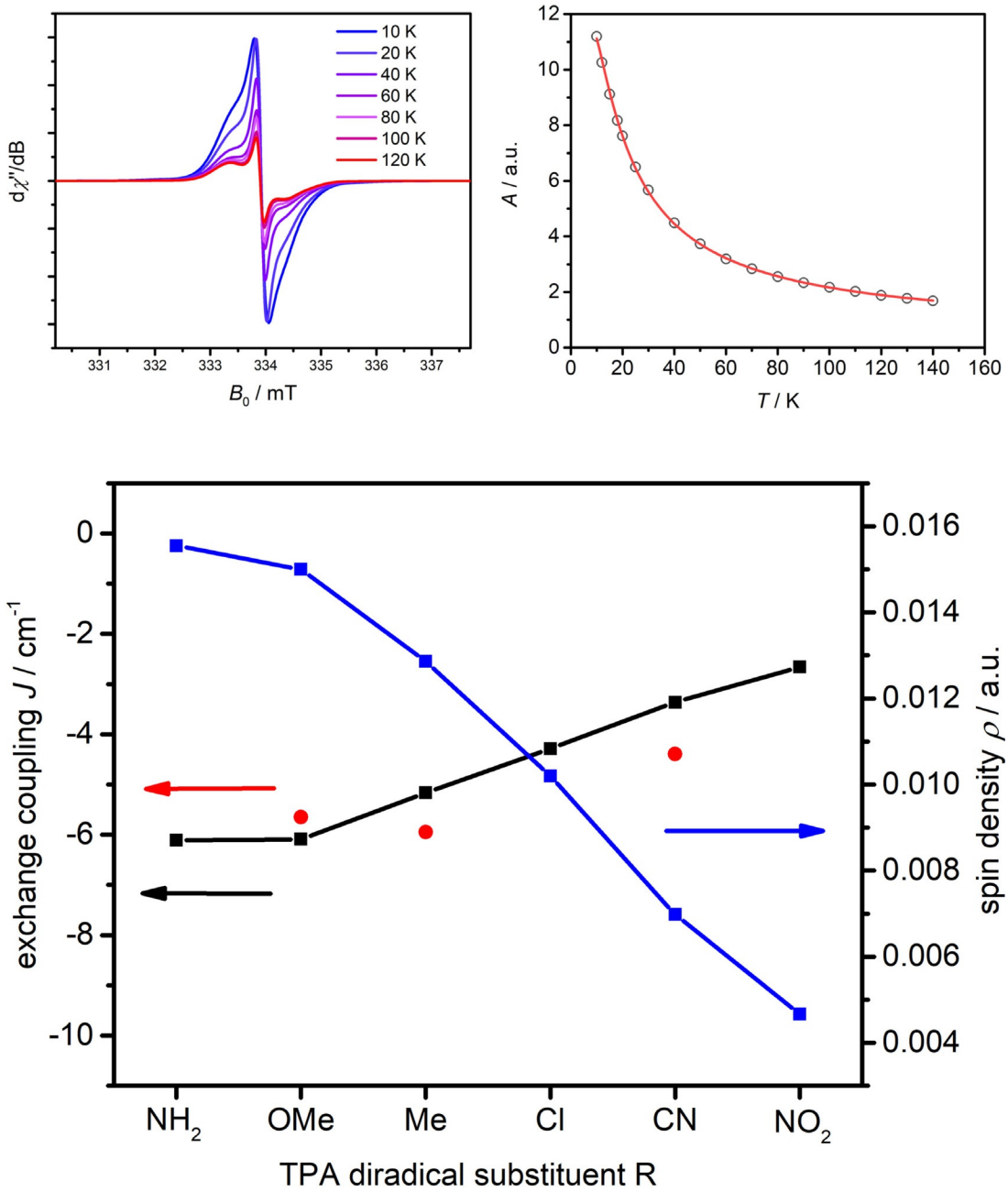

Figure 2. Top left) EPR spectra of **TPA(CN)(PyBTM″)$_2$** at different temperatures. Top right) Double integral of EPR spectra vs. temperature (circles) and fit by Bleaney–Bowers Equation (1) (red line). Bottom) Calculated (UCAMB3LYP/6-31G*) exchange coupling *J* (black), spin density at UB3LYP (blue) of the HS state and *J* experimental (red) coupling from temperature dependent EPR measurements for a series of TPA diradicals with varying substituent, R.

The temperature dependence of the double integral of the main signal of the TPA bridged diradicals (see Figure 2 and Table S1, Figure S3) were fitted with the Bleaney–Bowers Equation (1),[13] which describes the magnetic susceptibility of a two spin system. Energy differences between triplet and singlet levels were fitted as $\Delta E = 2J = -8.78\ \mathrm{cm}^{-1}$ for **TPA(CN)(PyBTM″)$_2$**, $2J = -11.9\ \mathrm{cm}^{-1}$ for **TPA(Me)(PyBTM″)$_2$**, and $2J = -11.3\ \mathrm{cm}^{-1}$ for **TPA(OMe)(PyBTM″)$_2$**, respectively. Here, *J* is the exchange interaction taken positive when the HS state is lower in energy than the LS state. For the **TPA(PyBTM″)$_3$** triradical, the magnetic susceptibility equation for triangular system (2)[14] was used and the energy difference between quartet and doublet levels was optimized as $3J = -14.3\ \mathrm{cm}^{-1}$. These small negative values can be interpreted as antiferromagnetic interactions between two spins or three spins inside a molecule, that is, in all cases the low spin state is slightly more stable. The order of absolute value of exchange interaction *J* [**(TPA(CN)(PyBTM″)$_2$** < **TPA(PyBTM″)$_3$** < **TPA(OMe)(PyBTM″)$_2$** < **TPA(Me)(PyBTM″)$_2$**] roughly follows the expected electron density on the N atom of TPA which are thought to mediate the interaction. Following a three-orbital superexchange model[15] with four electrons (two unpaired electrons and one

 © 2019 The Authors. Published by Wiley-VCH Verlag GmbH & Co. KGaA, Weinheim

electron pair at the bridge connecting the spin bearing orbitals, see Supporting Information), rising the energy of the bridge orbital (e.g., by donor substituents as in the TPA moiety) leads to an increase of the singly occupied MO constructed from the interaction of the three localized orbitals. This increase favours the antiferromagnetic contribution and leads to an increase of $|-J|$. Since the spin-spin interactions are not strong ($3J/k < 30$ K), both HS and LS states exist in almost equal amount for diradicals and triradicals at room temperature.

$$\chi_A = \frac{Ng^2\beta^2}{kT}\frac{1}{3+\exp(-2J/kT)} + N\alpha \quad (1)$$

$$\chi_A = \frac{Ng^2\beta^2}{12kT}\frac{5+\exp(-3J/kT)}{1+\exp(-3J/kT)} + N\alpha \quad (2)$$

Temperature dependence of the EPR signal strength of **TPB(PyBTM″)$_3$** in toluene showed an unexpected behavior at low temperature and the data points could not be fitted by Equations (1) or (2). However, a powder sample of **TPB(PyBTM″)$_3$** diluted in KBr gave a Bleaney–Bowers fit [Eq. (1)] with a large antiferromagnetic value (Table S2, Figure S4, $2J = -349$ cm^{-1}), and no meaningful fit was obtained with the equation for triangular system (2). The results indicate that in the solid state some intermolecular magnetic interactions are much stronger than intramolecular ones. Temperature dependence of the double integral of the signal of **TPB(Me)(PyBTM″)$_2$** in toluene was fitted by the Equation (1) with $2J = -16.2$ cm^{-1}. This value is remarkably high compared to those of the other diradicals. However, using the same superexchange model as described above but with only two unpaired electrons (because the boron p-orbital is empty), we arrive at the same conclusion that a low lying vacant bridge orbital increases the orbital energy gap and favors the antiferromagnetic state thereby increasing $|-J|$. This is one of the rare cases in organic chemistry where an empty orbital mediates the spin-spin interaction.

In order to verify the electronic structure of the compounds, the molecular structures were optimized by DFT calculations at the UB3LYP/6-31G* level for all possible spin multiplicities (see Supporting Information). However, because the wave function of the low spin state in all calculations was calculated by the "broken symmetry" approach and in fact represents a mixture of LS and HS state, the exact energy difference between the LS and the HS state was evaluated by Equation (3)[16] taking the spin expectation values into account. The thereby estimated J values depend strongly on the functional (see Figure S12) but using CAMB3LYP yielded reasonable agreement with the experiment for all TPA bridged radicals, that is, the LS state is always more stable than the HS state, see Figure 2c. Therein we also give the J values for some TPA derivatives with substituent R = NH_2, Cl, and NO_2 which have not been studied experimentally but which illustrate the influence of the TPA substituent clearly. The trend expected from the three-orbital superexchange model was indeed verified, that is, J varies smoothly along the electron donating (withdrawing) strength of the substituent at the TPA unit (R = NH_2, OMe, Me, Cl, CN, NO_2). The spin density at the TPA nitrogen also varies accordingly.

$$J = \frac{E_{LS} - E_{HS}}{\langle \hat{S}^2 \rangle_{HS} - \langle \hat{S}^2 \rangle_{LS}} \quad (3)$$

Calculated spin density distributions of the molecules are shown in Figure S13. In general, α-spin molecular orbital and β-spin molecular orbital are not degenerate for open-shell compounds such as radicals. While orbitals are delocalized by π-conjugation, the largest coefficients are on the radical carbon for the LUMOs, and on amine nitrogen for the HOMOs (see Figure 3 for an example, the orbitals of the other radicals can be found in Figure S14). These are the centers where reduction and oxidation occurs, respectively. There is one more α-spin electron than β-spin electron in the (doublet) monoradicals. In these cases, the lowest unoccupied molecular orbitals are β-spin orbitals (β-LUMOs), and the highest occupied molecular orbitals are α-spin orbitals (α-HOMOs).

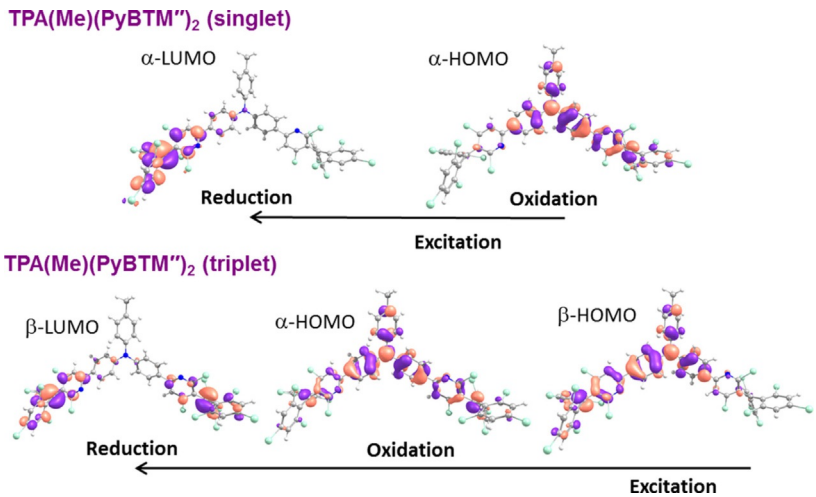

Figure 3. Frontier orbitals of singlet and triplet **TPA(Me)(PyBTM″)$_2$** calculated at the UB3LYP/6-31G* level. The orbital energy increases from right to left. See also Figure S14 for orbitals of the other radicals.

© 2019 The Authors. Published by Wiley-VCH Verlag GmbH & Co. KGaA, Weinheim

For the triplet diradicals with two excess α-electrons the LUMOs are β-LUMOs, and the HOMOs are α-HOMOs. In the singlet diradicals the number of α-spin electrons and β-spin electrons are the same, and α- and β-LUMOs, and α- and β-HOMOs are almost degenerate. The quartet triradicals behave similar to the triplet diradicals and the doublet triradicals similar to the singlet diradicals concerning the orbital energies. In all compounds irrespective of the spin, the lowest unoccupied molecular orbital is mainly located on the PyBTM″ groups. The highest occupied molecular orbitals of the TPA compounds are centered on the TPA moiety but show considerably delocalization onto the PyBTM″ groups in some compounds. In contrast, the highest occupied molecular orbitals of the TPB compounds are positioned on the PyBTM″ groups. These assignments correspond to the results obtained by electrochemistry analysis where first oxidation occurs at the amine in the TPA bridged radicals but at the PyBTM″ in TPB bridged radicals. Reduction and oxidation potentials and the calculated energies of the LUMOs and HOMOs correlated qualitatively (see Table S3).

Plotting the computed spin density (HS state) of the central nitrogen along with the exchange interaction *J* indicates that the central atom mediates the exchange interaction for the TPA compounds (see Figure 2c). The spin density is tuned by the electron donating or withdrawing substituent at the TPA.

Electronic spectra of all compounds show strong absorption around 25000–30000 cm^{-1} which is characteristic for chlorinated triarylmethyl radical compounds.[17] Furthermore, the TPA bridged radicals display somewhat weaker absorptions between 17000–25000 cm^{-1}, and even weaker lowest energy absorptions between 12000–19000 cm^{-1} (Figure 4). As the DFT calculation revealed (see below), this band consists of several transitions, one for the monoradicals, two for the diradicals and three for the triradicals. Therefore, it is difficult to give the energy of maximum absorption of the lowest energy band because of varying intensities of these overlapping bands. Thus, we evaluated the 00-energy by the intersection of a tangent at the low energy flank with the baseline (see Table 1). These lowest energy absorptions have to some extent CT character[18] and their maxima are shifted towards lower energy the stronger the donor is (see Figure 4a and 4b: **TPA(OMe)(PyBTM″)$_2$** > **TPA(Me)(PyBTM″)$_2$** > **TPA(CN)(PyBTM″)$_2$**) and the more radical centers are involved (see Figure 4c **TPA(CN)$_2$(PyBTM″)** > **TPA(CN)(PyBTM″)$_2$** > **TPA(PyBTM″)$_3$**). In general the absorption coefficients become larger as the number of PyBTM″ groups increases.

For the TPB compounds the lowest energy band is rather weak and shifted towards higher energy (see Figure 4d). Furthermore, there is a very strong absorption peaking at ca. 22000 cm^{-1} which is neither seen in unsubstituted triarylboranes[19] nor in the TPA compounds and thus has to be assigned to interactions of the triarylborane with the radical center.

While the assignment of bands is quite clear for the TPA compounds, the electronic nature of the lowest energy band and the very intense band of the boranes are unclear. Thus, the absorption spectra were calculated by TD-UDFT (UB3LYP/6-31G*) for both LS and HS state of the monoradicals, diradicals, and triradicals. The lowest excited state of the monoradical consists mainly of β-HOMO → β-LUMO transition (see TD-UDFT calculations in the Supporting Information). For the diradicals there are two almost degenerate excited singlet states

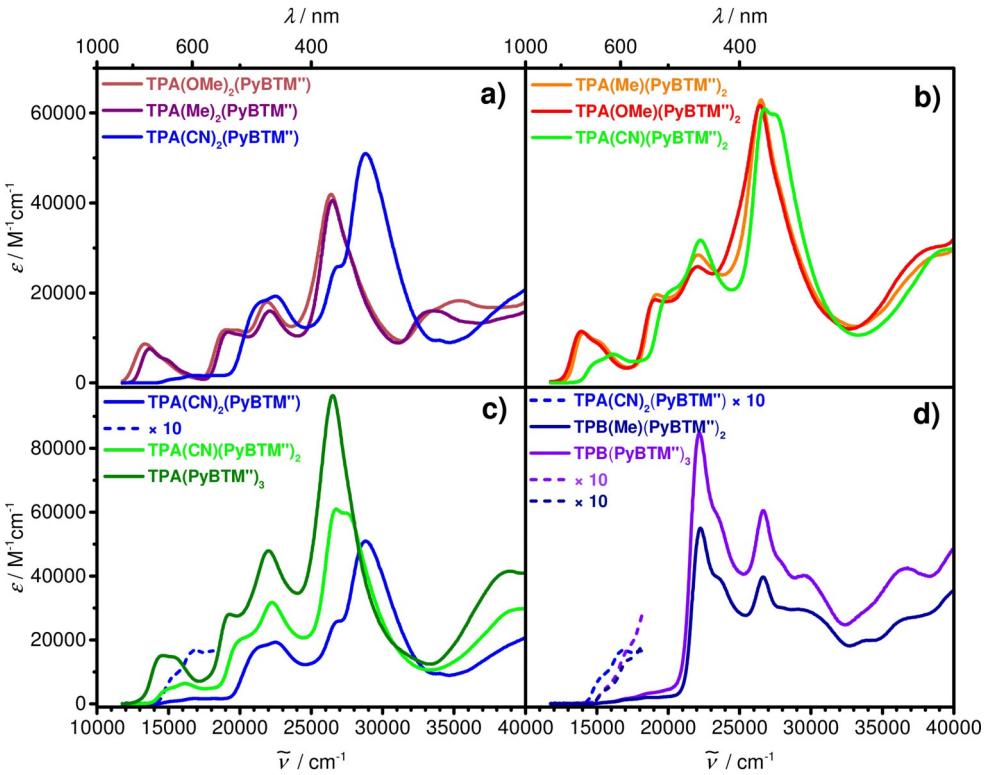

Figure 4. Absorption spectra of radicals in cyclohexane.

© 2019 The Authors. Published by Wiley-VCH Verlag GmbH & Co. KGaA, Weinheim

Table 1. Experimental (E_{00}) and TD-UDFT[a] computed lowest energy absorption data in the gas phase.

	E_{00}[b]/cm^{-1}	LS$_{cal}$/cm^{-1}[c]	f[d]	HS$_{cal}$/cm^{-1}[e]	f[d]
TPB(PyBTM″)$_3$	14800	15800	0.003	17900	0.072
		15800	0.005	18000	0.070
		16000	0.008	18200	0.001
		16100	0.002		
TPB(Me)(PyBTM″)$_2$	14800	15700	0.004	17900	0.099
		16000	0.005	18000	0.022
TPA(CN)$_2$(PyBTM″)	14400	15700	0.12		
TPA(CN)(PyBTM″)$_2$	14100	13900[f]	0.14	14500	0.25
		13900[f]	0.13	15200	0.061
TPA(PyBTM″)$_3$	13300	12600[f]	0.16	13600	0.24
		12900[f]	0.22	13600	0.25
		13600[f]	0.10	14700	0.00
TPA(Me)(PyBTM″)$_2$	13000	12300[f]	0.26	12700	0.29
		12500[f]	0.11	13500	0.053
TPA(OMe)(PyBTM″)$_2$	12700	12100[f]	0.33	12400	0.31
		12200[f]	0.06	13300	0.056
TPA(Me)$_2$(PyBTM″)	12600	12100	0.18		
TPA(OMe)$_2$(PyBTM″)	12000	11500	0.20		

[a] UB3LYP/6-31G*. [b] 00-energy obtained by the intersection of a tangent at the low energy flank of the lowest energy absorption band with the baseline. [c] Low spin state absorption energy. [d] Oscillator strength. [e] High spin state absorption energy. [f] Highly spin contaminated.

corresponding to α-HOMO → α-LUMO and β-HOMO → β-LUMO transitions and two excitations for the triplet state with β-HOMO → β-LUMO und β-HOMO → β-LUMO + 1 transitions. For the TPA bridged doublet triradical there are three excitations corresponding to α-HOMO → α-LUMO, β-HOMO → β-LUMO and β-HOMO → β-LUMO + 1 and also three excitations for the quartet states with β-HOMO → β-LUMO, β-HOMO → β-LUMO + 1 and β-HOMO → β-LUMO + 2. For the TPB bridged triradical there is a strong mixing of a large number of configurations for both doublet and quartet state.

For TPA compounds, both α- and β-HOMOs have the largest coefficients at the site of the amine nitrogen atom, and the lowest absorption transitions can be described as charge transfer absorptions from TPA to PyBTM″. The calculated excitation energies and oscillator strengths of the respective HS state are somewhat higher than that of the LS states (the difference is more pronounced for the boron compounds) but in general are in excellent agreement with the experimental E_{00} data (see Table 1) taking into account that the UDFT computations refer to vertical excitations.

Moreover, for both spin states of the TPA diradicals and the triradical, the transitions are highly allowed showing that the actual spin multiplicity of the ground state does not matter for the optical transitions because, unlike singlet closed shell ground state molecules, there are two ground states in the diradicals and triradicals.

For the boron bridged radical, the situation is somewhat different. From the fact that the boron p-orbital is vacant one clearly attributes acceptor character to the triarylborane which is at odd with the assignment of the lowest energy transition to a CT. However, the boron has significant σ-donor character which increases electron density in the aryl rings while the chlorines on the PyBTM″ Table 2 group have σ-acceptor character which decreases electron density in these aryl rings. Although the α-HOMO is on PyBTM″ radical, the β-HOMO is still located at the triarylborane aryl groups (see Supporting Information). Thus, despite the vacant boron-p-orbital there is enough electron density in the triarylborane to donate electron density to the very strong radical acceptor upon optical excitation which therefore can be assigned to a CT transition. Vice versa, according to the TD-UDFT computations, the high intensity transition at ca. 22000 cm^{-1} can be assigned to a reverse CT from the PyBTM″ radical center to the triarylborane acceptor (see Supporting Information).

All radicals display strong fluorescence in cyclohexane (Figure 5). Luminescence of TPA bridged radicals was quenched in more polar solvents such as dichloromethane similarly to the previous reports. The 00-energy of the radicals' fluorescence shows a distinct Stokes shift of ca. 800–1100 cm^{-1} (see Table 2) and thus displays the same trend as the absorp-

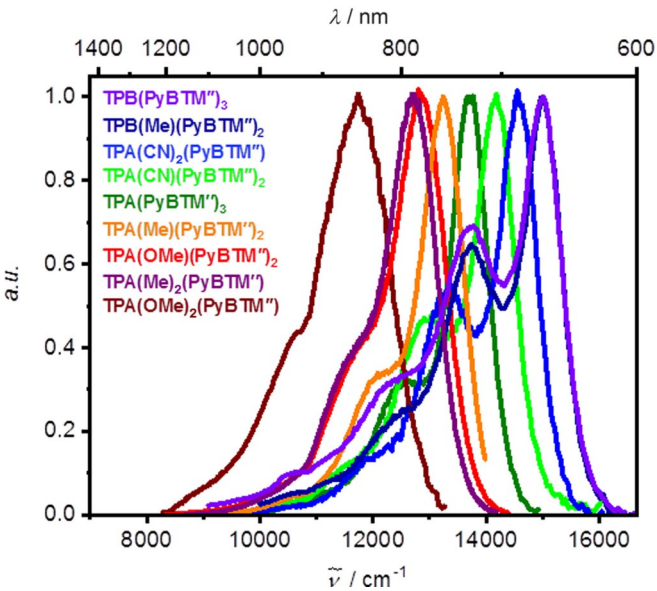

Figure 5. Fluorescence spectra of all radicals in cyclohexane at r.t.

Table 2. Emission properties of radical compounds.

	$\tilde{\nu}_{fl}$/ cm^{-1}	E_{00}[a]/ cm^{-1}	Φ/ %	τ/ns	k_f/ 10^7 s^{-1}	k_{nr}/ 10^7 s^{-1}
TPB(PyBTM″)$_3$	15000	15800	0.3	1.3	0.2	77
TPB(Me)(PyBTM″)$_2$	15000	15800	0.4	1.5	0.3	66
TPA(CN)$_2$(PyBTM″)	14500	15300	2.4	3.2	0.8	31
TPA(CN)(PyBTM″)$_2$	14200	14900	3.7	4.4[b]	0.8	22
TPA(PyBTM″)$_3$	13700	14400	6.1	5.8	1.1	16
TPA(Me)(PyBTM″)$_2$	13200	14000	7.9	7.2	1.1	13
TPA(OMe)(PyBTM″)$_2$	12900	13800	6.0	6.5	0.9	14
TPA(Me)$_2$(PyBTM″)	12700	13500	24	8.6	2.7	8.9
TPA(OMe)$_2$(PyBTM″)	11800	12800	2.8	1.9	1.5	51

[a] 00-Energy obtained by the intersection of a tangent at the low energy flank of the fluorescence band with the baseline. [b] Broadband fluorescence upconversion yields the following time constants: 7.5 ps, 99 ps and 3.5 ns.

© 2019 The Authors. Published by Wiley-VCH Verlag GmbH & Co. KGaA, Weinheim

tion maxima (see Table 1). Although the TPB core is a π-acceptor, the fluorescence bands fit in a continuous trend of the other donor-acceptor radicals supporting the argument that the TPA serves as a (weak) donor in combination with a strong radical acceptor.

One may ask as to what extent the small energy difference between the HS and LS excited state influences the fluorescence spectra. The almost identical shape of the emission spectra of **TPA(OMe)(PyBTM″)$_2$** and **TPA(Me)$_2$(PyBTM″)** clearly shows that the fact that the former compound may adopt two different spin states while the latter possesses only one has no influence on the shape of the emission band. Similar is true for **TPA(CN)(PyBTM″)$_2$** and **TPA(CN)$_2$(PyBTM″)**. We also measured the fluorescence lifetimes (τ) of all radicals by time-correlated single photon counting (TCSPC) at 15 240 cm^{-1} excitation (the boron bridged radicals at 19 420 cm^{-1}) and, in one case (**TPA(CN)(PyBTM″)$_2$**), by broadband fluorescence upconversion at 16 900 cm^{-1} excitation. In all cases, we found a monoexponential decay as given in Table 2. Even when measuring at emission energies lower than the fluorescence maximum the lifetimes are monoexponential. Only for the shortest times, the fluorescence upconversion spectra display weak band narrowing due to vibrational relaxation (see Figure S7). Furthermore, excitation spectra are in excellent agreement for different fluorescence detection energies. Transient absorption spectra of **TPA(CN)(PyBTM″)$_2$** at 16 100 cm^{-1} excitation with fs-time resolution corroborates the formation of a CT state by showing the typical signal for a triarylamine radical cation at ca. 13 300 cm^{-1} (see Figure S8) also did not give any hint for the population of two energetically different excited CT states. All these experiments show that fluorescence from the HS and the LS state are virtually identical and cannot be distinguished.

Absolute fluorescence quantum yields (Φ) of the radicals were determined by means of an integration sphere and are given in Table 2. The TPA compounds showed higher quantum yields and longer lifetimes than the TPB compounds with **TPA(Me)$_2$(PyBTM″)** possessing the highest quantum yield of 24%. For luminescent radicals, in which intersystem crossing does not play a role, the quantum yields are the result of a competition between rates of fluorescence (k_f) and non-radiative decay (k_{nr}) to the ground state (=internal conversion, IC). These quantities were calculated from quantum yields and lifetime via $k_f = \Phi/\tau$ and $k_{nr} = (1-\Phi/\tau)$, respectively. There are two reasons for enhancement of fluorescence by addition of TPA: increase of k_f and decrease of k_{nr}. Increase of k_f is explained by increase of oscillator strength of the transition between the ground state and the lowest excited state as can be seen by the intensity of the lowest energy absorption which is also reflected by the TD-UDFT calculations (Table 1); here the TPA bridged radicals have larger values of oscillator strengths and absorption coefficients than TPB bridged radicals. The value of k_{nr} was smallest for **TPA(Me)$_2$(PyBTM″)** and second smallest for **TPA(Me)(PyBTM″)$_2$**. Largest k_{nr} values for TPB bridged radicals and larger k_{nr} values for cyano radicals indicate that strong charge transfer from TPA to PyBTM″ promotes the radiative decay pathway. However, **TPA(OMe)$_2$(PyBTM″)** showed a large k_{nr} value, probably because of the lowest energy of the excited CT state (small D_0–D_1 gap).

Two-photon absorption (2PA)[20] induced fluorescence in the near infrared is a highly sought after property for biomarkers, bioimaging[21] and micro structuring.[22] Linear and branched acceptor–donor–acceptor type chromophores appear to be suitable design concepts. Therefore, we measured the 2PA cross section of **TPA(PyBTM″)$_3$**, **TPA(OMe)(PyBTM″)$_2$**, and **TPA(OMe)$_2$(PyBTM″)**, see Figure 6 (and Figure S11), in comparison to the 1PA cross section derived from the absorption spectra. While for the monoradical the 2PA cross section follows roughly the lowest energy absorption between 12 000–17 000 cm^{-1} and the peak at ca. 19 000 cm^{-1}, the 2PA cross section of the diradical and even more that of the triradical are significantly enhanced, reaching quite impressive 1000–3000 GM, particularly at around 19 000 and 15 500 cm^{-1}, which contrasts the behavior of recently investigated tris-(tetrachlorophenyl)methyl radicals.[6b] The latter signal shows that the lowest energy absorption band between 12 000–17 000 cm^{-1} is indeed composed of at least two or three electronic transitions. For example, assuming ideal D_3 symmetry in **TPA(PyBTM″)$_3$**, irrespective of the spin multiplicity, the two lowest energy excited states are (almost) degenerate and 1PA is allowed, but the third state at slightly higher energy is 1PA forbidden (see Table 1). In 2PA spectroscopy this is reversed. In reality, the selection rules are not that strict because of molecular distortion and vibrational coupling to asymmetric modes.[23] The enhancement of 2PA cross section of the triradical and the diradical vs. the monoradical cannot be explained by the simple additivity of individual chromophore moieties in the three radicals but must be caused by interactions between the three (two) donor-acceptor branches.

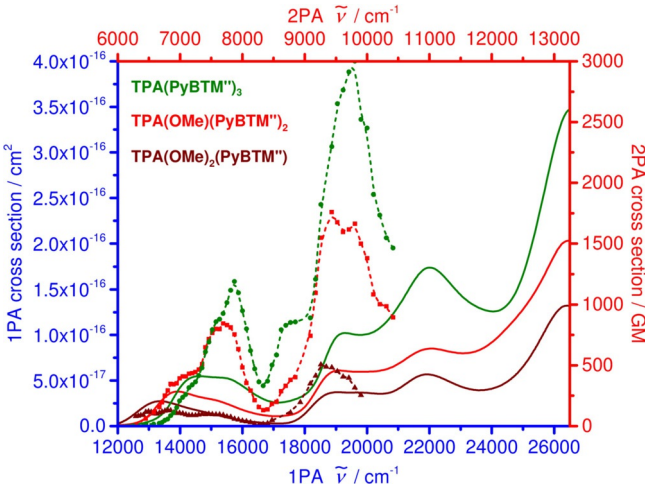

Figure 6. 1PA (solid lines) and 2PA (dashed lines) cross sections of selected radicals in cyclohexane solution.

Because of the good fluorescence properties we selected **TPA(OMe)(PyBTM″)$_2$** diradical as dopant for an OLED test device. This diradical is luminescent as guest in spin-coated PMMA or *p*-terphenyl thin film matrices despite the slight po-

© 2019 The Authors. Published by Wiley-VCH Verlag GmbH & Co. KGaA, Weinheim

larity of the hosts (see Figure S9). When photo-exciting an OLED (ITO/PEDOT:PSS/PDY-132 + TPA(OMe)(PyBTM″)$_2$/Ca/Al) at 532 nm the photoluminescence of PDY-132 (Super-Yellow from Merck) is strongly quenched by the **TPA(OMe)(PyBTM″)$_2$** dopant indicating an highly efficient Förster resonance energy transfer (Figure S10). Upon electrical excitation of the OLEDs, luminescence of **TPA(OMe)(PyBTM″)$_2$** was clearly observed for voltages above 8 V (Figure 7), demonstrating that, as a proof-of-concept, NIR OLEDs can be built from diradicals. As Ai and co-workers pointed out,[3b] this might also be advantageous concerning the spin statistics of exciton formation in OLEDs but in-depth investigation in this direction requires knowledge on the efficiency of the contributing populations and emission channels which is beyond the scope of this work.

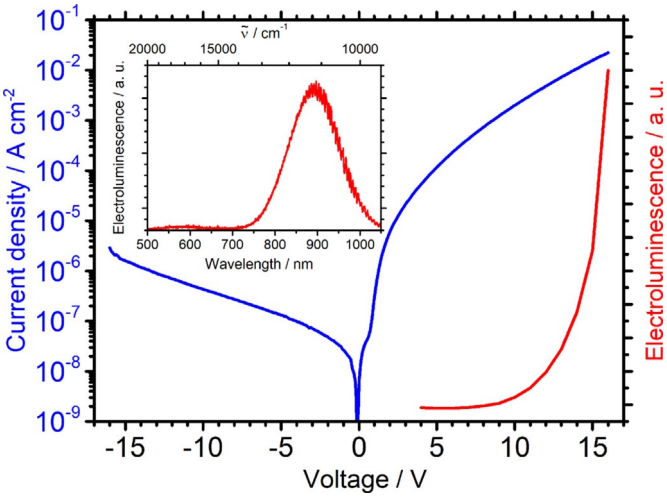

Figure 7. Current density and electroluminescence vs. applied voltage for an ITO/PEDOT:PSS/PDY-132 + **TPA(OMe)(PyBTM″)$_2$**/Ca/Al OLED device. Inset: electroluminescence spectrum recorded at 14 V.

Conclusion

In summary, mono-, di-, triradicals with significant fluorescence ranging from the red visible to NIR region were synthesized. The lowest excited states are charge transfer states for both the TPA and the TPB bridged radicals. While the HS and LS spin states are almost degenerate for the di- and triradicals, their actual spin multiplicity has almost no influence on the photophysics thereby rendering weakly coupled diradicals useful emitting species for two-photon applications and particularly for NIR OLED devices where spin statistics need to be considered.

Acknowledgements

This work was supported by the Deutsche Forschungsgemeinschaft (GRK 2112) and by a JSPS Overseas Research Fellowships to Y.H.

Conflict of interest

The authors declare no conflict of interest.

Keywords: density functional calculations · fluorescence · NIR OLED · radical · two-photon absorption

[1] a) Y. Beldjoudi, M. A. Nascimento, Y. J. Cho, H. Yu, H. Aziz, D. Tonouchi, K. Eguchi, M. M. Matsushita, K. Awaga, I. Osorio-Roman, C. P. Constantinides, J. M. Rawson, *J. Am. Chem. Soc.* **2018**, *140*, 6260; b) S. R. Ruberu, M. A. Fox, *J. Phys. Chem.* **1993**, *97*, 143; c) N. J. Reilly, D. L. Kokkin, M. Nakajima, K. Nauta, S. H. Kable, T. W. Schmidt, *J. Am. Chem. Soc.* **2008**, *130*, 3137; d) N. J. Reilly, M. Nakajima, T. P. Troy, N. Chalyavi, K. A. Duncan, K. Nauta, S. H. Kable, T. W. Schmidt, *J. Am. Chem. Soc.* **2009**, *131*, 13423; e) Y. Hattori, T. Kusamoto, H. Nishihara, *Angew. Chem. Int. Ed.* **2014**, *53*, 11845; *Angew. Chem.* **2014**, *126*, 12039; f) S. Kimura, T. Kusamoto, S. Kimura, K. Kato, Y. Teki, H. Nishihara, *Angew. Chem. Int. Ed.* **2018**, *57*, 12711; *Angew. Chem.* **2018**, *130*, 12893; g) Y. Hattori, T. Kusamoto, H. Nishihara, *RSC Adv.* **2015**, *5*, 64802; h) R. Beaulac, G. Bussiere, C. Reber, C. Lescop, D. Luneau, *New J. Chem.* **2003**, *27*, 1200.

[2] a) M. López, D. Velasco, F. Lopez-Calahorra, L. Julia, *Tetrahedron Lett.* **2008**, *49*, 5196; b) D. Velasco, S. Castellanos, M. Lopez, F. Lopez-Calahorra, E. Brillas, L. Julia, *J. Org. Chem.* **2007**, *72*, 7523; c) L. Fajarí, R. Papoular, M. Reig, E. Brillas, J. L. Jorda, O. Vallcorba, J. Rius, D. Velasco, L. Julia, *J. Org. Chem.* **2014**, *79*, 1771; d) A. Heckmann, S. Dümmler, J. Pauli, M. Margraf, J. Köhler, D. Stich, C. Lambert, I. Fischer, U. Resch-Genger, *J. Phys. Chem. C* **2009**, *113*, 20958; e) V. Gamero, D. Velasco, S. Latorre, F. Lopez-Calahorra, E. Brillas, L. Julia, *Tetrahedron Lett.* **2006**, *47*, 2305; f) M. Souto, H. Cui, M. Pena-Alvarez, V. G. Baonza, H. O. Jeschke, M. Tomic, R. Valenti, D. Blasi, I. Ratera, C. Rovira, J. Veciana, *J. Am. Chem. Soc.* **2016**, *138*, 11517.

[3] a) Q. Peng, A. Obolda, M. Zhang, F. Li, *Angew. Chem. Int. Ed.* **2015**, *54*, 7091; *Angew. Chem.* **2015**, *127*, 7197; b) X. Ai, E. W. Evans, S. Dong, A. J. Gillett, H. Guo, Y. Chen, T. J. H. Hele, R. H. Friend, F. Li, *Nature* **2018**, *563*, 536.

[4] H. Braunschweig, S. Ghosh, J. O. C. Jimenez-Halla, J. H. Klein, C. Lambert, K. Radacki, A. Steffen, A. Vargas, J. Wahler, *Chem. Eur. J.* **2015**, *21*, 210.

[5] D. Reitzenstein, T. Quast, F. Kanal, M. Kullmann, S. Rützel, M. S. Hammer, C. Deibel, V. Dyakonov, T. Brixner, C. Lambert, *Chem. Mater.* **2010**, *22*, 6641.

[6] a) S. Castellanos, F. López-Calahorra, E. Brillas, L. Juliá, D. Velasco, *Angew. Chem. Int. Ed.* **2009**, *48*, 6516–6519; *Angew. Chem.* **2009**, *121*, 6638; b) X. Wu, J. O. Kim, S. Medina, F. J. Ramirez, P. Mayorga Burrezo, S. Wu, Z. L. Lim, C. Lambert, J. Casado, D. Kim, J. Wu, *Chem. Eur. J.* **2017**, *23*, 7698; c) M. Steeger, S. Griesbeck, A. Schmiedel, M. Holzapfel, I. Krummenacher, H. Braunschweig, C. Lambert, *Phys. Chem. Chem. Phys.* **2015**, *17*, 11848.

[7] a) X. Hu, W. Wang, D. Wang, Y. Zheng, *J. Mater. Chem. C* **2018**, *6*, 11232; b) Y. Ni, J. Wu, *Tetrahedron Lett.* **2016**, *57*, 5426; c) F. Hinkel, J. Freudenberg, U. H. F. Bunz, *Angew. Chem. Int. Ed.* **2016**, *55*, 9830; *Angew. Chem.* **2016**, *128*, 9984; d) Z. Zeng, X. Shi, C. Chi, J. T. Lopez Navarrete, J. Casado, J. Wu, *Chem. Soc. Rev.* **2015**, *44*, 6578; e) N. M. Gallagher, A. Olankitwanit, A. Rajca, *J. Org. Chem.* **2015**, *80*, 1291; f) I. Ratera, J. Veciana, *Chem. Soc. Rev.* **2012**, *41*, 303; g) C. Lambert, *Angew. Chem. Int. Ed.* **2011**, *50*, 1756; *Angew. Chem.* **2011**, *123*, 1794.

[8] a) J. Fabian, R. Zahradník, *Angew. Chem. Int. Ed. Engl.* **1989**, *28*, 677; *Angew. Chem.* **1989**, *101*, 693; b) Y. Ni, S. Lee, M. Son, N. Aratani, M. Ishida, A. Samanta, H. Yamada, Y.-T. Chang, H. Furuta, D. Kim, J. Wu, *Angew. Chem. Int. Ed.* **2016**, *55*, 2815; *Angew. Chem.* **2016**, *128*, 2865; c) M. Abe, *Chem. Rev.* **2013**, *113*, 7011.

[9] Y. Hattori, S. Kimura, T. Kusamoto, H. Maeda, H. Nishihara, *Chem. Commun.* **2018**, *54*, 615.

[10] a) L. Ji, S. Griesbeck, T. B. Marder, *Chem. Sci.* **2017**, *8*, 846; b) C. D. Entwistle, T. B. Marder, *Angew. Chem. Int. Ed.* **2002**, *41*, 2927; *Angew. Chem.* **2002**, *114*, 3051.

[11] Because of the helicity of the triarylmethyl radical, triarylamine and triarylborane moieties, as well as of the conformation of the pyridyl group relative to the adjacent phenylene rings, all compounds studied in this

© 2019 The Authors. Published by Wiley-VCH Verlag GmbH & Co. KGaA, Weinheim

work form diverse diastereoisomers which interconvert slowly on the NMR time scale as can be seen by, for example, two proton signals for the pyridyl group. Therefore, all characterizations made in this work refer to a mixture of diastereosiomers.

[12] a) G. Gryn'ova, D. L. Marshall, S. J. Blanksby, M. L. Coote, *Nat. Chem.* **2013**, *5*, 474; b) T. Kusamoto, S. Kume, H. Nishihara, *J. Am. Chem. Soc.* **2008**, *130*, 13844.

[13] B. Bleaney, K. D. Bowers, *Proc. R. Soc. London Ser. A* **1952**, *214*, 451.

[14] H. Okawa, M. Mikuriya, S. Kida, *Bull. Chem. Soc. Jpn.* **1983**, *56*, 2142.

[15] a) P. J. Hay, J. C. Thibeault, R. Hoffmann, *J. Am. Chem. Soc.* **1975**, *97*, 4884; b) J. P. Launay, M. Verdaguer, "The localized electron: magnetic properties" in *Electrons in Molecules*, Oxford University Press, Oxford, **2014**.

[16] a) T. Soda, Y. Kitagawa, T. Onishi, Y. Takano, Y. Shigeta, H. Nagao, Y. Yoshioka, K. Yamaguchi, *Chem. Phys. Lett.* **2000**, *319*, 223; b) L. Noodleman, *J. Chem. Phys.* **1981**, *74*, 5737; c) N. Ferré, N. Guihery, J.-P. Malrieu, *Phys. Chem. Chem. Phys.* **2015**, *17*, 14375.

[17] a) M. Ballester, J. Riera, J. Castaner, C. Badia, J. M. Monso, *J. Am. Chem. Soc.* **1971**, *93*, 2215; b) O. Armet, J. Veciana, C. Rovira, J. Riera, J. Castaner, E. Molins, J. Rius, C. Miravitlles, S. Olivella, J. Brichfeus, *J. Phys. Chem.* **1987**, *91*, 5608.

[18] M. Kaupp, M. Renz, M. Parthey, M. Stolte, F. Würthner, C. Lambert, *Phys. Chem. Chem. Phys.* **2011**, *13*, 16973.

[19] a) C. D. Entwistle, T. B. Marder, *Chem. Mater.* **2004**, *16*, 4574; b) M. Kinoshita, H. Kita, Y. Shirota, *Adv. Funct. Mater.* **2002**, *12*, 780.

[20] a) F. Terenziani, C. Katan, E. Badaeva, S. Tretiak, M. Blanchard-Desce, *Adv. Mater.* **2008**, *20*, 4641; b) G. S. He, L.-S. Tan, Q. Zheng, P. N. Prasad, *Chem. Rev.* **2008**, *108*, 1245; c) M. Pawlicki, H. A. Collins, R. G. Denning, H. L. Anderson, *Angew. Chem. Int. Ed.* **2009**, *48*, 3244; *Angew. Chem.* **2009**, *121*, 3292.

[21] a) H. M. Kim, B. R. Cho, *Chem. Rev.* **2015**, *115*, 5014; b) W. Denk, J. H. Strickler, W. W. Webb, *Science* **1990**, *248*, 73; c) P. Ning, W. Wang, M. Chen, Y. Feng, X. Meng, *Chin. Chem. Lett.* **2017**, *28*, 1943; d) Q. Zhang, X. Tian, H. Zhou, J. Wu, Y. Tian, *Materials* **2017**, *10*, 223.

[22] a) B. H. Cumpston, S. P. Ananthavel, S. Barlow, D. L. Dyer, J. E. Ehrlich, L. L. Erskine, A. A. Heikal, S. M. Kuebler, I. Y. S. Lee, D. McCord-Maughon, J. Qin, H. Rockel, M. Rumi, X.-L. Wu, S. R. Marder, J. W. Perry, *Nature* **1999**, *398*, 51; b) S. Kawata, H.-B. Sun, T. Tianaka, K. Takada, *Nature* **2001**, *412*, 697; c) W. Zhou, S. M. Kuebler, K. L. Braun, T. Yu, J. K. Cammack, C. K. Ober, J. W. Perry, S. R. Marder, *Science* **2002**, *296*, 1106; d) S. Juodkazis, V. Mizeikis, H. Misawa, *J. Appl. Phys.* **2009**, *106*, 051101.

[23] a) D. Scherer, R. Dörfler, A. Feldner, T. Vogtmann, M. Schwörer, U. Lawrentz, W. Grahn, C. Lambert, *Chem. Phys.* **2002**, *279*, 179; b) B. Strehmel, S. Amthor, J. Schelter, C. Lambert, *ChemPhysChem* **2005**, *6*, 893.

Manuscript received: June 28, 2019
Version of record online: November 19, 2019

 © 2019 The Authors. Published by Wiley-VCH Verlag GmbH & Co. KGaA, Weinheim